Journal of Biomolecular NMR **29:** 477–490, 2004.

Experiments for correlating quaternary carbons in RNA bases

Radovan Fiala*, Markéta L. Munzarová & Vladimír Sklenář*
National Centre for Biomolecular Research, Masaryk University, Kotlářská 2, 611 37 Brno, Czech Republic

Received 10 December 2003; Accepted 15 April 2004

Key words: ab initio, correlation, DFT, NMR, quaternary carbon, RNA, spin-spin coupling

Abstract

The paper presents a set of triple-resonance two-dimensional experiments for correlating all quaternary carbons in RNA bases to one or more of the base protons. The experiments make use of either three-bond proton-carbon couplings and one selective INEPT step (the long-range selective HSQC experiment) to transfer the magnetization between a proton and the carbon of interest and back, or they rely on one- and/or two-bond heteronuclear (the H(CN)C and H(N)C experiments) or carbon-carbon (the H(C)C experiment) couplings and multiple INEPT transfer steps. The effect of the large one-bond carbon-carbon coupling in t_1 is removed by a constant time evolution or by a selective refocusing. The performance of the proposed approach is demonstrated on a 0.5 mM 25-mer RNA. The results show that the experiments are applicable to samples containing agents for weak molecular alignment. The design of the correlation experiments has been supported by *ab initio* calculations of scalar spin-spin couplings in the free bases and the AU and GC base pairs. The *ab initio* data reveal surprisingly high values of guanine $^2J_{N1C5}$ and uracil $^2J_{N3C5}$ couplings that are in a qualitative agreement with the experimental data. The sensitivity of the spin-spin couplings to base pairing as well as the agreement with the experiment depend strongly on the type of nuclei involved and the number of bonds separating them.

Abbreviations: HSQC – heteronuclear single-quantum correlation; INEPT – insensitive nuclei enhancement by polarization transfer; RDC – residual dipolar coupling; DFT – density functional theory.

Introduction

Nucleic acids are compounds of fundamental importance. During the past decade NMR spectroscopy benefited from the development of innovative tools and greatly improved its ability to study the RNA (and DNA) structure using advanced methods of isotopically-assisted multi-dimensional spectroscopy. Although ^{13}C and ^{15}N isotopes have become essential for resolving spectra of larger RNAs, the proton NOE data still provide the crucial information for an accurate structure determination. The low proton density in nucleic acids, however, poses a problem in the structure refinement. Six poorly resolved protons found in the RNA ribose moiety, and only one or two non-exchangeable protons in the purine and the pyrimidine bases, produce a limited number of conformationally dependent NOEs. To characterize the structure of a nucleic acid with a good accuracy, it is therefore highly important to supplement the proton NOE data with additional constraints.

Since the advent of methods for isotopic labeling of RNA's in the early 1990's, an astonishing variety of increasingly sophisticated heteronuclear experiments has been proposed. The new methods enabled an unambiguous assignment of resonances based on the through-bond sugar-to-base correlations (Hu et al., 2001; Phan, 2001; Fiala et al., 2000; Krishnamurthy, 1996; Sklenář et al., 1993, 1994; Farmer et al., 1994), the identification of imino protons in loop and bulge regions by establishing their through-bond connectivities to the non-exchangeable protons (Wohnert et al., 1999, 2003; Phan, 2000; Simorre et al., 1996; Sklenář et al., 1996; Fiala et al., 1996), and the direct obser-

*To whom correspondence should be addressed. E-mails: {fiala, sklenar}@ncbr.chemi.muni.cz

vation of hydrogen bonds in nucleic acid base pairs (Majumdar et al., 2001; Majumdar and Patel, 2002; Pervushin et al., 1998; Pervushin, 2001; Dingley and Grzesiek, 1998).

To increase the number of available constraints, novel experiments relying on residual anisotropic interactions observed in the solution containing media for a partial alignment have been introduced (Boisbouvier et al., 2003; Hennig et al., 2001; Richter et al., 2000; Wu et al., 2001a, b; Yan et al., 2002; Žídek et al., 2001). In addition to easily measurable one-bond ^{1}H-^{13}C and ^{1}H-^{15}N, and long-range ^{1}H-^{1}H and ^{1}H-^{31}P RDCs, also two-bond ^{1}H-^{13}C and ^{1}H-^{15}N, as well as one-bond ^{13}C-^{15}N interactions can provide valuable information. As demonstrated, their values, measured with a sufficiently high precision, can be successfully applied to the structure refinement of nucleic acids (Padrta et al., 2002). The changes of the ^{31}P isotropic shifts observed in the aligned state have also been used as constraints in the structure calculations of DNA (Wu et al., 2003).

The NOE data together with the torsion angles and the RDCs form the basic pool of constraints for a structure calculation. In contrast to proteins, only a few attempts have been made to decipher the relationship between the chemical shifts and the secondary and tertiary structure of nucleic acids and to utilize the chemical shifts as a source of structural information. (Wijmenga et al., 1997; Altona et al., 2000; Cromsigt et al., 2001).

The proton chemical shifts, as well as the chemical shifts of ^{13}C and ^{15}N nuclei directly attached to protons, are readily available from the assigned ^{1}H-^{13}C and ^{1}H-^{15}N one-bond correlation spectra. Also chemical shifts of the glycosidic nitrogens can be obtained from two- or three-dimensional experiments correlating the sugar H1′ and base H8/H6 protons. So far, however, little attention has been paid to study the quaternary carbons in nucleic acid bases. Potentially, their chemical shifts could be applied as a valuable restraint. Since the number of quaternary carbons exceeds the number of carbons with directly bonded hydrogens, it is highly desirable to develop a strategy for their detection. Here we propose a set of experiments that allow sensitive measurements of all quaternary carbons in purine and pyrimidine bases. Since the direct assignment of quaternary carbons is virtually impossible, their signals are correlated with nuclei that can be assigned from other sources.

The heteronuclear correlation experiments are typically based on the polarization transfer through scalar couplings. The nuclei in pyrimidine and purine bases form a rather complicated network of coupled spins. The experimental values of most of the couplings, but not all of them, are known (Wijmenga and van Buuren, 1998). To supplement the experimental values and to resolve some ambiguities in the available data we have performed *ab initio* calculations of the spin-spin couplings in optimized GC and AU pairs as well as in each of the RNA bases. The sensitivity of couplings to base pairing and comparison with the experimental data are discussed.

Materials and methods

Theoretical values of scalar spin-spin coupling constants have been determined for the A, G, C, U bases and the AU, GC base pairs substituted on N1 (pyrimidine) and N9 (purine) by methyl groups. Molecular geometries have been optimized in Kohn-Sham calculations with the B3LYP functional (Becke, 1988, 1993) and the 6-31G(d) basis (Hehre et al., 1972; Frisch et al., 1984) in the implementation of Gaussian 98 (Frisch et al., 1998). C_s symmetry has been imposed and default convergence criteria applied. Spin-spin coupling constants were calculated by a combined SOS-DFPT (for the PSO and DSO terms) and DFT/FPT (for the FC term) approach as implemented in the deMon-NMR code (Malkin et al., 1994a, b; Salahub et al., 1991). The SD (spin-dipolar) term has been neglected in the present approach for the following reasons: (a) This term is – especially for a longer-range coupling – relatively small; (b) it is in most cases smaller than the error in the DFT calculation of the FC term; and (c) it represents the most time-consuming step of nuclear spin-spin coupling calculations at the DFT level (Malkin et al., 1994a, b; Salahub et al., 1991). The density functional calculations employed Perdew and Wang's GGA for exchange (Perdew and Wang, 1986) in combination with Perdew's GGA for correlation (Perdew, 1986a, b). The orbital basis set IGLO-III (Kutzelnigg et al., 1990) in combination with the corresponding experimental auxiliary basis was used for all atoms. The convergence criteria were set to 1.0×10^{-6} Hartree (energy) and to 1.0×10^{-5} (density). The numerical grid was specified as RADI64/FINE. The level-shifting parameter was set to 3.0 eV for isolated bases and to 5.0 eV for base pairs.

The FC contribution to J_{MN} has been for all M, N computed with a finite perturbation of $\lambda = 0.001$ first centered on nucleus M and then on nucleus N. Whereas for the hypothetical case of an exact

Table 1. Experimental parameters

Experiment	Pulse sequence[a]	^{1}H sw[b] [ppm]	^{13}C sw[b] [ppm]	^{13}C frq[c] [ppm]	^{15}N frq[c] [ppm]	τ^{a} [ms]	$\Delta^{a}_{(1)}$ [ms]	Δ^{a}_{2} [ms]	CT[d] [ms]	NS/NI[e]	ET[f] [h]
Adenine H2/8-C4 LR-HSQC		10.0	15.0	149.0	202.0	32.00				128/64	4
Adenine H2-C6 LR-HSQC		10.0	15.0	156.0	220.0	28.00				128/64	4
Purine H8-C5 LR-HSQC		10.0	16.5	118.0	202.0	26.00				128/64	4
Purine H8-C4 HCC	a	10.0	20.0	143.0	202.0	2.30	28.0		15.0	128/64	4
Purine H8-C4 HCNC	c	10.0	15.0	149.0	170.0	2.30	26.0	30.0	15.0	128/64	4
Pyrimidine H6-C2 LR-HSQC		10.0	15.0	154.0	149.0	28.00				128/64	4
Pyrimidine H6-C2 HCNC	c	10.0	15.0	154.0	149.0	2.76	26.0	30.0		128/64	4
Pyrimidine H6-C4 LR-HSQC		10.0	15.0	166.5	170.0	28.00				128/64	4
Pyrimidine H5-C4 HCC	a	10.0	15.0	166.5	150.0	2.70	8.3		16.6	128/64	4
Guanine H1-C2 HNC	b	20.0	19.5	151.6	140.0	5.56	22.0			64/128	4
Guanine H1-C6 HNC	b	20.0	30.0	161.5	140.0	5.56	28.0		11.4	64/128	4
Guanine H1-C5 HNC	b, d	20.0	19.5	118.0	140.0	5.56	25.0			64/128	4
Uracil H3-C2 HNC	b	20.0	16.6	152.0	158.0	5.56	24.0			16/128	1
Uracil H3-C4 HNC	b	20.0	30.0	169.0	158.0	5.56	30.0		15.3	64/128	4
Uracil H3-C5 HNC	b	20.0	30.0	105.0	158.0	5.56	50.0		15.3	64/128	4

[a]Refer to Figure 2.
[b]Spectral width.
[c]Transmitter frequency.
[d]Constant time interval; if no value is given either a simple t_1 evolution (correlations of the C2 carbons) or the selective refocusing (Figure 2d) was used.
[e]Number of scans per FID collected (NS) and number of increments (NI, real + imaginary FIDs).
[f]Total experimental time (rounded).

exchange-correlation functional and an exact numerical procedure the results would not depend on the origin of the FPT perturbation, in real calculations the FC term does depend on the perturbation center. For more than 90% of the computed couplings, the difference in J_{MN} upon switching the center of perturbation turned out smaller than 0.10 Hz. For the rest of J_{MN}, involving especially $^{1}J_{CN}$ and $^{1}J_{CC}$ – type couplings, the difference was between 0.10 and 0.20 Hz, with a few extreme outliers of 0.2–0.4 Hz. Theoretical scalar couplings reported below represent the arithmetic average of the values for the two nuclei perturbed. The difference in J_{MN} upon switching the center of perturbation could be in some cases reduced by improving the SCF convergence and both values converged to the same average value as obtained with the less stringent convergence criteria.

All spectra were measured on a 0.5 mM 25-mer RNA construct related to the trypanosome U6 intramolecular stem-loop with a sequence of GGGUCUCCCUGCGCAAGGCUGAUCG. The samples contained 50 mM NaCl at pH 6.8 and were fully ^{13}C and ^{15}N labeled on either A and U residues or G and C residues. The measurements were performed at 298 K on a Bruker 600 MHz Avance spectrometer at 14.1 T equipped with a triple resonance (^{1}H, ^{13}C, ^{15}N) probe. 1024 points in the ^{1}H dimension were acquired. The GARP decoupling (Shaka et al., 1985) was applied during the acquisition with the power of 1.84 kHz and 980 Hz on ^{13}C and ^{15}N, respectively. Either 64 scans and 64 complex increments (for the correlations with the exchangeable protons) or 128 scans and 32 complex increments (the other experiments) were collected resulting in the experimental time of approximately four hours per spectrum. The only exception was the Uracil H3-C2 correlation measured with 16 scans, where the data was collected within one hour. The data sets were processed in XWIN-NMR program into 1k × 1k matrices using square cosine apodization in both dimensions and the deconvolution of the residual water peak (Marion et al., 1989). Other experimental parameters are summarized in Table 1. The details on frequency selective pulses are given in the corresponding figure captions. The spectra were referenced indirectly to DSS in both ^{1}H and ^{13}C dimensions, the referencing was based on the chemical shift of the water resonance (Wishart et al., 1995).

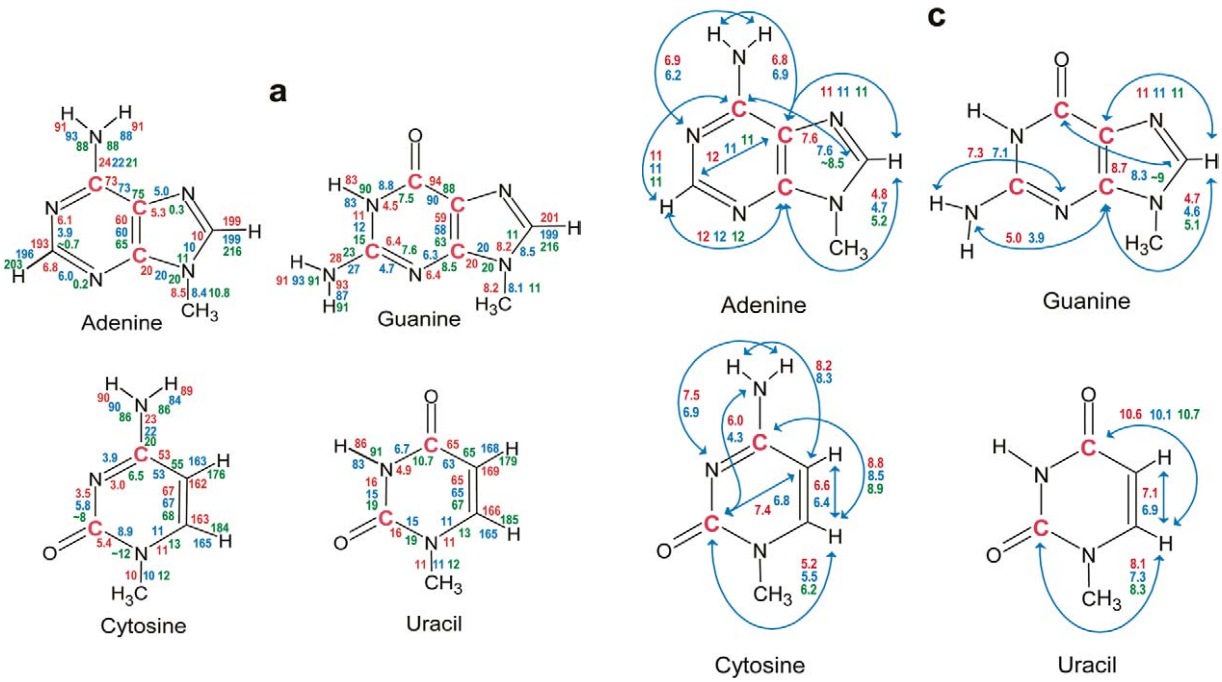

Figure 1. Absolute values of relevant (excluding oxygen) couplings in RNA bases across one (a), two (b), and three (c) bonds. The figures shown in red and blue are theoretical values for the bases and the base pairs, respectively, calculated as described in the text. The green numbers are experimental values (Wijmenga and van Buuren, 1998). Only the couplings for which at least one of the three absolute values exceeded 5 Hz are given; a complete list of theoretical couplings (including signs) is available as Supplementary material.

Results and discussion

Selected absolute values of *ab initio* spin-spin coupling constants in RNA bases and base pairs are presented in Figure 1, along with the available experimental data for AMP, GMP, UMP and CMP (Wijmenga and van Buuren, 1998). A complete list of theoretical and experimental data is available as Supplementary Material. Throughout this section, the theoretical data obtained for RNA bases will be compared to those obtained for RNA base pairs in order to provide the reader with an estimate of the base-pairing effects on the couplings. Both sets of theoretical data will then be used for a detailed, quantitative comparison to the available experimental data for mononuclosides (Wijmenga and van Buuren, 1998) for the purposes of both validating the theory and estimating the influence of the environment on the studied couplings. A qualitative comparison will also be presented between the theoretical results and our experimental data for RNA base pairs.

The comparison of the theoretical and experimental results reveals a few general features: (1) There is a significant influence of base pairing on the intrabase spin-spin couplings. (2) The sensitivity to base pairing and the agreement with experiment depend strongly on the type of nuclei involved and the number

of bonds separating them. Particular types of coupling reveal similar performance for all bases in question. (3) In many cases, the experimental data obtained for mononucleosides compare better to the theoretical data for the base pairs than to those for isolated bases. This fact, however surprising at the first sight, can be well rationalized as follows: The experimental measurements for mononucleosides have been performed in solutions where the polar groups of bases are expected to participate in similar kind of interactions as formed in base pairs. These interactions are absent in calculations performed on the bases *in vacuo*, but some (of course a very rough and incomplete) account of them is apparently taken in calculations performed for base pairs. An explicit study of the influence of solvent on the spin-spin coupling constants is beyond the scope of this work but represents a next logical step in comparing theoretical and experimental results. For an evaluation, we have divided the couplings into five groups based on the differences between the calculated and experimental coupling values.

*Theoretical couplings within 10% or 1 Hz of experiment for both isolated bases and base pairs**

This class of results, little dependent on base pairing and comparing very well to experiment, comprises 20 out of 26 C-H couplings and 12 out of 15 C-C couplings. The theoretical values are in most cases slightly underestimated with respect to the experiment.** Same agreement with the experiment is obtained also for all N-H couplings over 1 or 3 bonds. On the other hand, only a minority (4 out of 46) of nitrogen-to-heavy atom couplings belong here. These outcomes are understandable considering that (a) nitrogen as a lone-pair bearing atom is more challenging for the DFT description of the spin-spin coupling (Malkin et al., 1994b), and (b) the couplings involving nitrogen turned out much more sensitive to base pairing than others. In many cases, very good to good agreement of theory with experiment is found for the base-pairs but is not obtained for the isolated bases (cf. below).

*This criterion is motivated by the fact that it is more difficult to obtain given relative agreement with experiment for small couplings than for large couplings. Also, many experimental couplings are not known with higher precision than $\sim$1 Hz.

**Any comparisons and/or evaluations of the coupling constants in this paper are based on their absolute values.

Theoretical couplings within 20% or 2 Hz of experiment for both isolated bases and base pairs

This class of results, relatively little dependent on base pairing and comparing well/reasonably to experiment, comprises (a) several C-H couplings involving C6(C,U) or H6(C,U); (b) all N-H couplings over 2 bonds; (c) nitrogen-heavy atom couplings, especially one-bond couplings between a carbon and a nitrogen that doesn't directly participate in the base pairing. The worse agreement with the experiment encountered for the couplings with C6(C,U) and H6(C,U) as compared to the rest of the C-H couplings (cf. above) can be attributed to specific solvent-solute interactions or possibly to the absence of the sugar in the theoretical model. In the pyrimidine nucleosides, a $\sigma_{H1'\text{-}C1'} \rightarrow \pi^*_{\text{N1-C6}}$ hyperconjugative interaction was found to influence significantly the C6-H1′ coupling (Munzarová and Sklenář, 2002). Other couplings with C6 may also be influenced by this interaction whose proper account requires a more realistic description of the C1′ bonding environment. It is also graspable that the N-H couplings over 2 bonds are more difficult to reproduce than those over 1 or 3 bonds. In general, the 2-bond spin-spin couplings may adopt a very wide spectrum of values depending on a delicate balance of positive and negative contributions. They thus more often challenge the theoretical treatment.

Theoretical couplings deviating from experiment by more than 20% and 2 Hz for both isolated bases and base pairs

The agreement between theory and experiment is problematic in this group. Nevertheless, the theoretical values are in most cases useful for a qualitative interpretation of experimental data. The lack of quantitative agreement can be most probably attributed to the failure of DFT and/or the presence of solvent effects of other types than base pairing. Besides $^2J_{\text{C4C8}}$(A, G), $^2J_{\text{N3N9}}$(A), and $^2J_{\text{N9C5}}$(G) this class of couplings comprises one-bond nitrogen-carbon couplings. Some of these couplings are significantly improved by base pairing as compared to experiment (especially $^1J_{\text{N1C2}}$ whose magnitude changes by 1 Hz for G, 2.2 Hz for A, and as much as 3.5 Hz for C) but the agreement is still below the 20% or 2 Hz threshold.

Theoretical couplings within 10% or 1Hz of experiment for isolated bases deviating from experiment by more than 10% and 1 Hz for the base

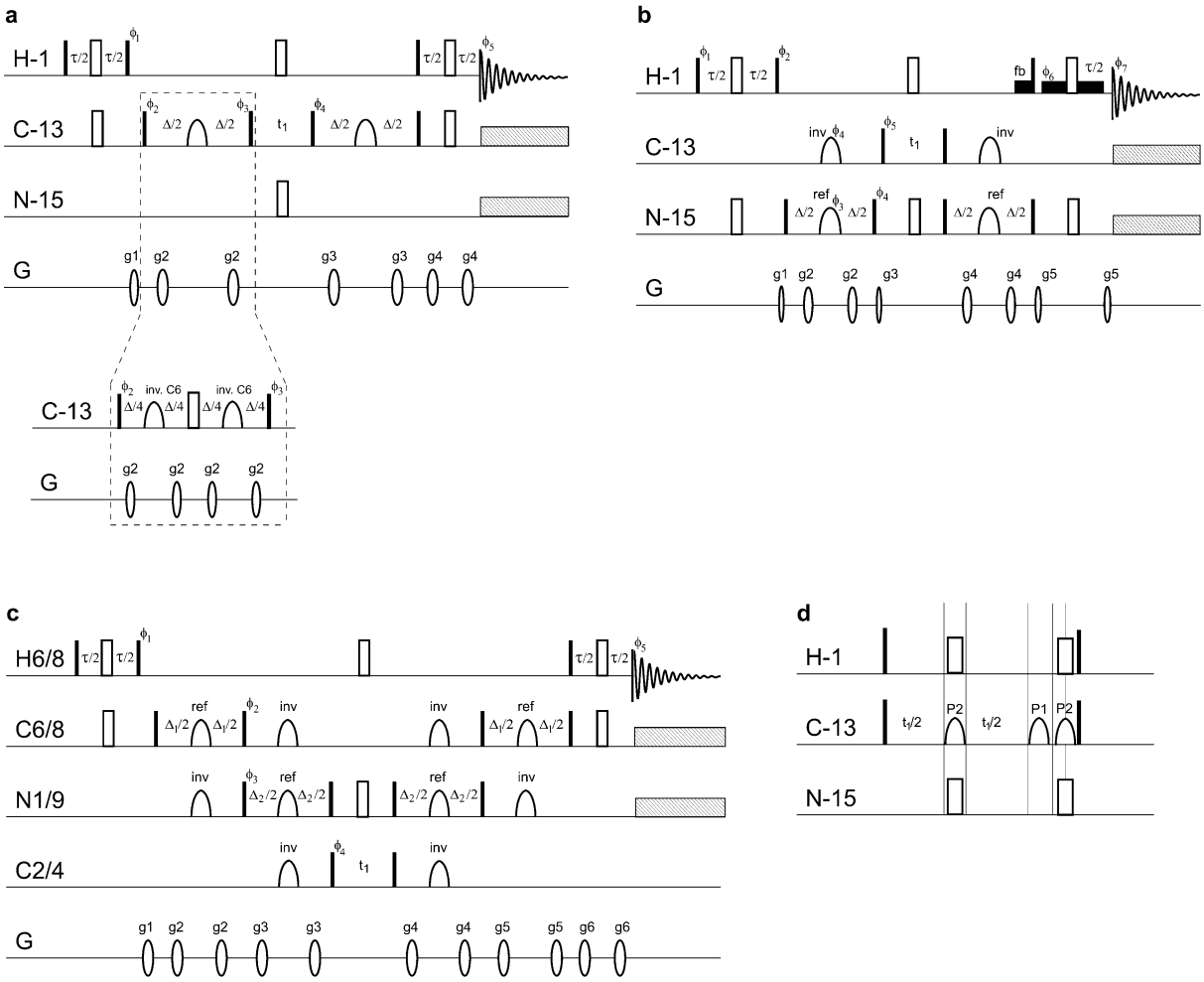

Figure 2. Schematic representations of the pulse sequences used: HCC for purine H8-C8-C4 (main figure) or pyrimidine H5-C5-C4 (inset) correlation (a), HNC (b) and HCNC (c). The solid bars and open rectangles represent nonselective 90° and 180° pulses, respectively, the half-elliptic symbols stand for frequency selective refocusing (ref) or inversion (inv) pulses, low solid rectangles are low power 90° square flip-back (fb) or WATERGATE pulses and elliptical symbols represent pulsed field gradients. If necessary, the splitting due to the large one bond carbon-carbon coupling can be eliminated using a constant time evolution period, refocused using selective pulses (d) or removed by a carbon homonuclear decoupling. P2 represents a selective inversion pulse applied to the coupling partner; P1 is a refocusing pulse selective to the studied carbon nucleus. If the period for refocusing carbon-proton antiphase magnetization is too short to accommodate the WATERGATE water suppression scheme, it can be extended by offsetting the proton and carbon 180° pulses. For details on the shaped pulses used in the individual experiments, see the captions to the corresponding spectra. All gradients are used for purging purposes only and need not be in any specific ratios. Phase cycles: HCC, $\phi_1 = y, -y$, $\phi_2 = x, x, -x, -x$ + States-TPPI, $\phi_3 = 4y, 4(-y)$ + States-TPPI, $\phi_4 = y$, $\phi_5 = x, -x, -x, x$; HNC, $\phi_1 = x, -x$, $\phi_2 = y, -y$, $\phi_3 = 4x, 4y, 4(-x), 4(-y)$, $\phi_4 = 16x, 16(-x)$, $\phi_5 = x, x, -x, -x$ + States-TPPI, $\phi_6 = -x$, $\phi_7 =$ a b a b b a b a where a = x, −x, −x, x and b = −x, x, x, −x; HCNC, $\phi_1 = y, -y$, $\phi_2 = y$, $\phi_3 = x, x, -x, -x$, $\phi_4 = 4x, 4(-x)$ + States-TPPI, $\phi_5 = x, -x, -x, x, -x, x, x, -x$. The other experimental parameters are summarized in Table 1.

pairs, and theoretical couplings within 20% or 2 Hz of experiment for isolated bases deviating from experiment by more than 20% and 2 Hz for the base pairs

This case is encountered only for $^1J_{N3C2}$(G) and $^1J_{N1C2}$ (U).

Theoretical couplings within 10% or 1 Hz of experiment for the base pairs deviating from experiment by more than 10% and 1 Hz for isolated bases, and theoretical couplings within 20% or 2 Hz of experiment for the base pairs deviating from

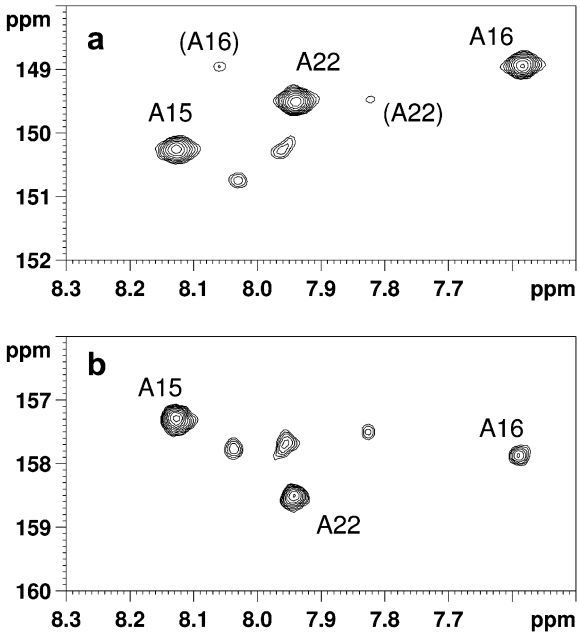

Figure 3. Adenine H2(H8)-C4 (a) and H2-C6 (b) correlations using the selective long-range HSQC experiment. The H8-C4 correlations (labeled in parentheses) show significantly reduced sensitivity due to a smaller value of the H8-C4 coupling. Unlabeled peaks come from impurities produced by partial decomposition of the sample. The selective magnetization transfer was achieved by inverting the C4, C5 or C6 carbon using 3.75 ms IBURP2 pulses (Geen and Freeman, 1991) in the middle of the evolution period. A 2.5 ms REBURP pulse (Geen and Freeman, 1991) shifted to 8 ppm refocuses the aromatic protons in the 7–9 ppm range. A 2.5 ms REBURP pulse and 2.5 ms IBURP2 inversion pulses shifted to 118 ppm were applied during the t_1 period to decouple the carbon-carbon interactions. For other experimental parameters, see Table 1.

experiment by more than 20% and 2 Hz for isolated bases

This kind of performance applies to $^{3}J_{C2C5}$(G) and 14 couplings involving imino nitrogens N1 (A,G) and N3 (C,U), and amino nitrogens N6, N2, N4 of A, G, C, respectively. The most illustrative examples are $^{2}J_{N1N6}$(A), $^{2}J_{N3N4}$(C), $^{1}J_{N1C6}$(A) where base pairing shifts the couplings towards a 10% or 1 Hz agreement with the experiment, and $^{2}J_{N2N3}$(G), $^{1}J_{N3C5}$(U) where a 20% or 2 Hz agreement is obtained. Still better comparison is obtained for the latter coupling when the experimental results for the base pair (5.8 Hz to 8.4 Hz, cf. below) are considered.

The efficiency of a correlation experiment involving multiple coherence transfer steps depends on interplay between the magnitudes of the coupling constants and the relaxation properties of the spins along the coherence transfer pathway. For the coupling to be useful for polarization transfer in molecules of realistic size (10 to 40 residues) and at typical concentrations ($\sim$ 1 mM), its value should be at least 5 Hz, preferably significantly larger. Based on the existing couplings we have found four different experiments capable of establishing correlations of quaternary carbons with protons in RNA bases.

1. The HSQC experiment utilizing long-range ^{1}H-^{13}C couplings. The selective proton refocusing and carbon inversion pulses direct the polarization transfer to the desired location. Theoretically, it is possible to correlate one proton with more quaternary carbons in a single experiment, e.g. H6 with C2 and C4 in pyrimidines. However, splitting the proton magnetization into two pathways reduces the sensitivity significantly.

2. In the H(C)C experiment (Figure 2a, the letters in parentheses refer to the nuclei whose chemical shifts are not recorded), the magnetization is transferred from a proton to the directly attached carbon followed by a carbon-carbon step via one-bond or a long-range carbon-carbon coupling. Note that this experiment differs from the original HCCH-COSY experiment (Kay et al., 1990) by returning the magnetization back to the original proton for detection. An experiment similar to ours, under the name of TROSY relayed HCCH-COSY, was used to correlate H2 to H8 protons in adenine via C4/C5/C6 carbons (Simon et al., 2001). In a nonselective fashion, all correlations were obtained in one experiment at the price that the magnetization was split into several pathways, resulting in a diminished sensitivity. The sequence was proposed as a 3D experiment in order to avoid fortuitous cancellation of signals with opposite sign. Our approach differs by a systematic use of carbon selective pulses in a strictly two-dimensional mode. As there is no evolution period for C2/8 carbons, the TROSY procedure cannot be applied for the sensitivity enhancement. Either one bond (pyrimidine H5-**C5-C4**) or long-range carbon-carbon couplings (purine H8-**C8-C4/6**) are employed for the carbon-carbon polarization transfer.

3. The H(N)C experiment (Figure 2b) is a variation of HNCA/HNCO experiments (Muhandiram and Kay, 1994) developed for protein backbone assignment. In nucleic acid bases, it can be used to correlate the imino proton of guanine or uracil to carbons that exhibit a significant coupling to the imino nitrogen such as guanine C2 and C4.

4. The H(CN)C experiment (Figure 2c) involves magnetization transfer from a proton to the directly attached carbon followed by two consecutive carbon-

nitrogen INEPT steps via one-bond C-N couplings. The pulse sequence adds an extra N-C step to the H(C)N experiment used previously for correlating H1' and H8 to N9 in purine nucleotides. The H(CN)C experiment can be used to correlate purine H8 with C4 and pyrimidine H6 with C2. On the other hand, purine N7 couplings to its neighboring carbons are too small to be useful for polarization transfer.

With the exception of pyrimidine and purine C2 carbons, all the base quaternary carbons exhibit a large one-bond carbon-carbon coupling. Moreover, the purine carbons are also subject to long-range carbon-carbon couplings of the order of 10 Hz. To obtain the best sensitivity and resolution, all couplings to the carbon of interest should be suppressed during the t_1 evolution period. For carbon-carbon couplings, this can be achieved using either a constant-time evolution or by a selective refocusing of the coupling partner's magnetization (Figure 2d). The rather large values of carbon-carbon coupling constants in the range of approximately 63 to 88 Hz limit the t_1 evolution time and consequently also the resolution in the carbon dimension if constant-time evolution is employed. An extension of the constant time period to 2/J or larger is not practical due to multiple long-range carbon-carbon couplings ranging from 5 to 12 Hz that would cause severe attenuation of the signal. For example the guanine C4 couplings of 8 Hz and 9.5 Hz to C8 and C6, respectively, cause a loss of signal of about 17% if a constant-time period of 15.6 ms is used. Extending the constant-time period to 31.2 ms (2/J) would lead to the loss of almost 58% of the signal. If the carbon of interest is coupled to two other carbons with different coupling constants, as in the case of purine C5, a compromised value of constant time, further limiting the sensitivity, has to be chosen. Therefore, an alternative approach of selective decoupling of the carbon-carbon interaction should be considered (Figure 2d). In this approach, a selective inversion pulse is applied to the coupling partner of the nucleus studied. The P1 refocusing pulse manipulates the nucleus of interest and eliminates the phase shift acquired during the long selective pulse employed in the t_1 period. The second P2 pulse removes the additional spin-spin interaction that would otherwise evolve during the refocusing period. Additional benefit of using two selective inversion P2 pulses is the suppression of the Bloch-Siegert shift. A prerequisite for the described selective decoupling of the carbon-carbon interaction is that the chemical shifts of the nuclei involved are sufficiently different so that the selective pulses can be applied to one nucleus without affecting the other. Alternatively, the carbon-carbon interaction could be removed by multiple-band-selective homonuclear ^{13}C decoupling during t_1 evolution interval using a decoupling sequence consisting of a train of adiabatic inversion pulses (Brutscher et al., 2001).

The experiments that involve carbon-attached protons can be performed in ^2H_2O solution with presaturation of the residual water resonance. The H(N)C experiment, on the other hand, involves imino protons that are in a fast exchange regime with the solvent and therefore has to be measured in H_2O solution. Suppression of the strong water signal can be achieved using WATERGATE (Piotto et al., 1992) solvent suppression scheme. To increase the workflow, however, it is preferable to avoid manipulations with the sample and measure all spectra in 90% H_2O/10% ^2H_2O solution. In the experiments relying on the non-exchangeable protons, presaturation of water resonance can be used. In the HSQC spectra, the water presaturation reduces the water signal sufficiently since the selective proton inversion pulses do not refocus the water resonance and virtually all the transverse magnetization of water is eliminated by the gradients during the last evolution period. In H(C)C and H(CN)C experiments, however, the proton 180° pulses are non-selective, the water magnetization is refocused and results in an excessive water signal. Therefore, additional solvent suppression by WATERGATE is necessary in the last evolution periods of the pulse sequences. Since the $\tau/2$ delays (Figures 2a, c) are only about 1.25 ms for the aromatic H-C couplings, it may not be possible to accommodate the selective WATERGATE pulses, the gradient pulses and the necessary recovery delays. If this is the case, the available delay can be extended by offsetting the proton and carbon 180° pulses. The extension should be kept at a necessary minimum to limit further loss of a signal due to relaxation. To minimize the effect of the saturation transfer arising from the chemical exchange and/or cross-relaxation, the water magnetization can be restored to the $+z$ axis before acquisition by a flip-back pulse (Grzesiek and Bax, 1993).

The carbons C4, C5, and C6 are quaternary in both adenine and guanine. In guanine, the C2 carbon is also quaternary while in adenine it caries a proton and it appears in one-bond ^1H–^{13}C HSQC spectrum. Since all adenine quaternary carbons exhibit a coupling larger that 10 Hz with either H2 or H8, it is rather straightforward to obtain the H2-C4 (Figure 3a), the H2-C6 (Figure 3b) and the H8-C5 (Figure 4a) correl-

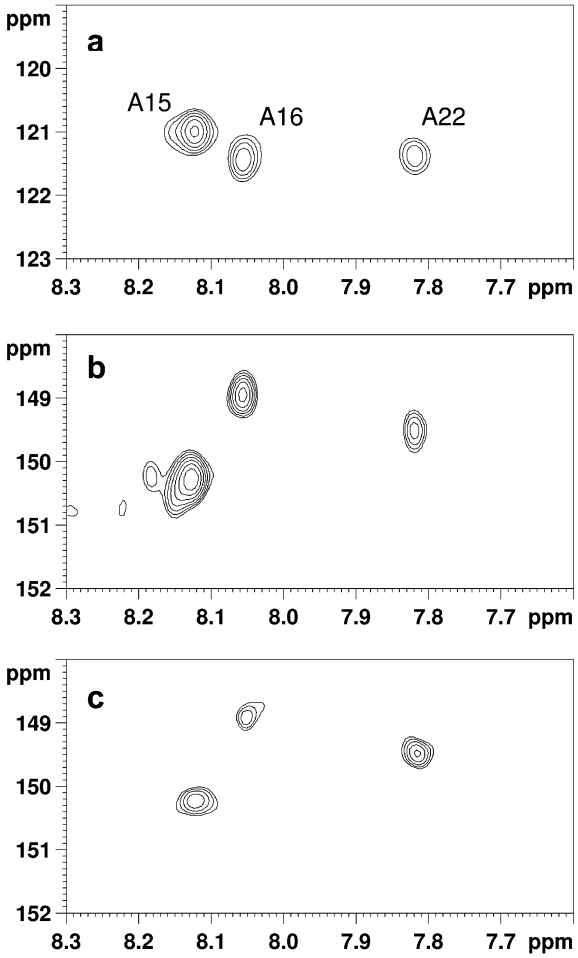

Figure 4. Adenine H8-C5 (a) correlation using the selective long-range HSQC experiment and adenine H8-C4 correlations using the HCC (b) and HCNC (c) experiments. The selective pulses were used as follows: (a) same as in Figure 3 except for 1.7 ms IBURP2 inversion pulses shifted to 155 ppm applied during the t_1 period, (b) 700 μs Q3 (Emsley and Bodenhausen, 1992) carbon pulses at 143 ppm, (c) 2.5 ms REBURP at 137 ppm for refocusing of the carbon C8, 1.05 ms IBURP2 at 143 ppm for inversion of the carbons C8 and C4, 4.2 ms REBURP for the nitrogen N9 refocusing and 4.2 ms IBURP2 for the nitrogen N9 inversion. For other experimental parameters, see Table 1.

ations using the long range HSQC experiment. Since the resonance of the C5 carbon is far from that of C4 and C6, the carbon-carbon couplings can be readily removed by using a selective inversion pulse on C5 (for C4 or C6 correlation experiments) or C4 and C6 (for C5 correlation) during the t_1 period (Figure 2d). This method is preferable to a constant time evolution especially with the C5 correlation experiment because of the different values of the $^1J_{C4C5}$ and $^1J_{C5C6}$ couplings as well as a presence of long range couplings.

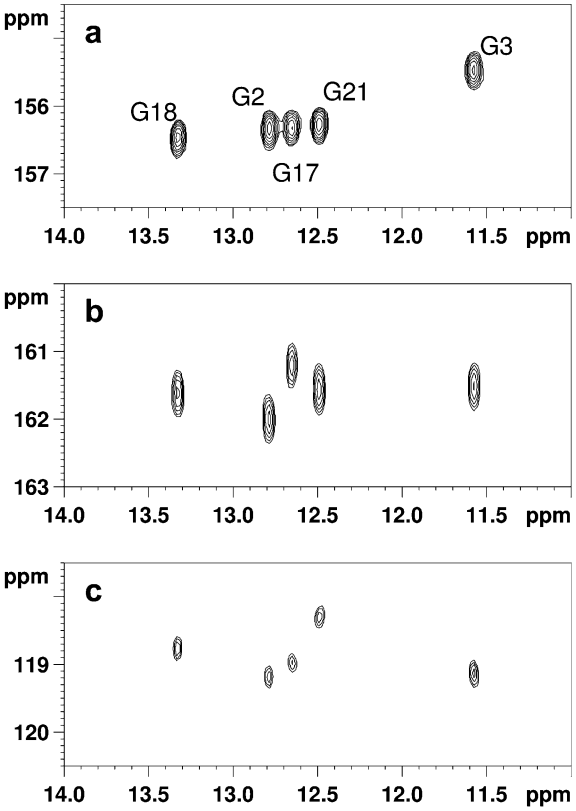

Figure 5. Guanine H1-C2 (a), H1-C4 (b) and H1-C5(c) correlations using the HNC experiment. In the middle of the Δ evolution periods, 1.2 ms Q3 gaussian cascades and 3.75 ms IBURP2 pulses were applied to nitrogen and carbon, respectively. The selective pulses in the t_1 period of the H1-C5 experiment (c) were applied as described for the H8-C5 correlation experiment. For other experimental parameters, see Table 1.

As expected, the H2-C4, H2-C6 and H8-C5 correlation experiments are quite sensitive thanks to relatively large coupling values of about 11 Hz. Besides the main coherences, some supplementary transfers may appear in the spectra, namely pyrimidine H6-C2 correlations in purine H2-C4 spectra or residual H2-C2 one-bond correlations in H2-C6 spectra. If desired, the supplementary correlations can be avoided or significantly reduced by using more selective carbon pulses, provided the resonance frequencies of the carbons are known with sufficient accuracy.

The H8-C4 peaks appear in the same experiment as the adenine H2-C4 correlations (Figure 3a), however, the peak intensities are significantly reduced due to a much smaller H8-C4 coupling of 5.2 Hz. A more sensitive way of obtaining the H8-C4 correlation is the H(C)C experiment (Figure 2a) that relies on consecutive polarization transfers via the large one bond

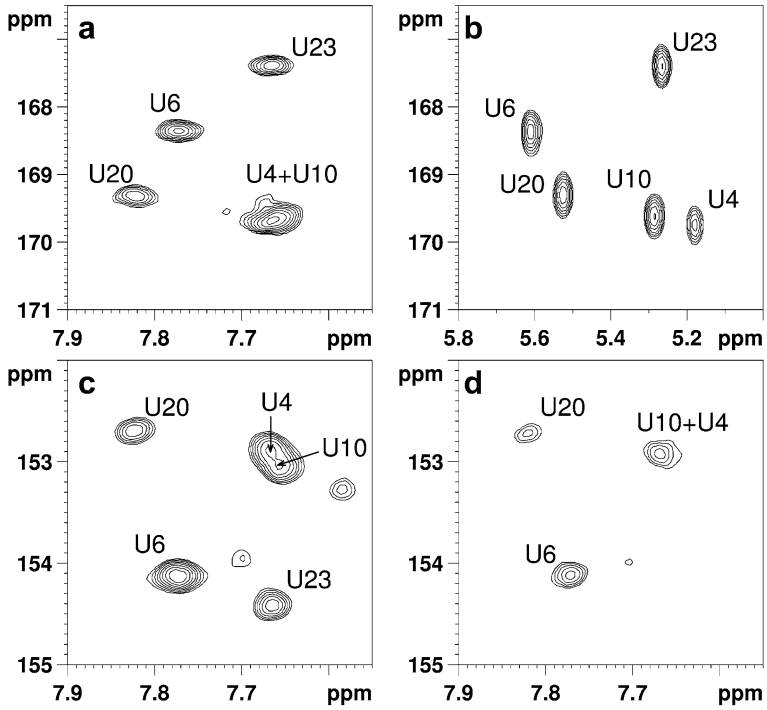

Figure 6. Pyrimidine C4 carbon correlated to H6 (a) and H5 (b) protons using selective long-range HSQC and HCC experiments, respectively, H6-C2 correlations using selective long-range HSQC (c) and HCNC (d) experiments. The selective pulses were used as follows: (a) same as in Figure 3 except the C5 inversion pulse was applied at 99 ppm, (b) C6 carbon inversion by 2.5 ms IBURP2 pulses at 140 ppm, (c) 2.0 ms Q3 pulse for the proton refocusing and a 2.5 ms IBURP2 pulse for the carbon inversion in the middle of the evolution period, (d) 2.5 ms REBURP at 140 ppm for refocusing of the carbon C6, 1.05 ms IBURP2 at 147 ppm for inversion of carbons C6 and C2, 4.2 ms REBURP for the nitrogen N1 refocusing and 4.2 ms IBURP2 for the nitrogen N1 inversion. For other experimental parameters, see Table 1.

H8-C8 coupling (215 Hz) and the C8-C4 coupling (∼8 Hz). Considering the relaxation properties of the molecule, 28 ms evolution intervals were chosen. The selective ^{13}C pulses must refocus the C8 magnetization and invert the C4 magnetization at the same time. It is therefore important to use pulses that exhibit good performance for both refocusing and inversion, such as the Q3 Gaussian cascades (Emsley and Bodenhausen, 1992). Since residual H8-C8 and H2-C2 peaks also appear in the spectrum, the spectral width in the ^{13}C dimension has to be set to include these regions. For this reason, a short t_1 evolution period dictated by the constant-time evolution is not a serious obstacle. The spectrum provides the best sensitivity of all H8-C4 correlation experiments (Figure 4b). A shorter carbon selective pulse shifted slightly downfield to cover the guanine C6 resonance frequencies provides a spectrum with simultaneous H8-C4 and H8-C6 correlations with a lower sensitivity due to the splitting of the magnetization into two pathways. However, we found this experiment to be useful only for those guanine residues whose imino protons cannot be detected due to the broadening. The other guanine C6 carbons can be correlated with the H1 proton (cf. below) with both superior sensitivity and chemical shift dispersion in the proton dimension, while the chemical shifts of adenine C6 carbons can be more easily measured from the H2-C6 correlation.

In the H(CN)C experiment the magnetization is transferred via the N9 nitrogen whose resonance (166–172 ppm) is well separated from all the other ^{15}N resonances in RNA bases. The spectra obtained using this experiment are very 'clean' – only purine H8-C4 peaks appear. The sensitivity of the experiment is comparable to the LR-HSQC (Figure 4c).

From the point of view of the H8 correlation experiments, the situation in guanine is essentially similar to adenine. Guanine lacks the H2 proton but unlike adenine its N1 nitrogen carries an imino proton. Direct couplings of the imino proton to any quaternary carbons are rather small, however. Instead, we can use moderately sized couplings of the imino nitrogen to its neighboring carbons C2 and C6 in the HNC experiment (Figure 2b). Interestingly, the DFT calcu-

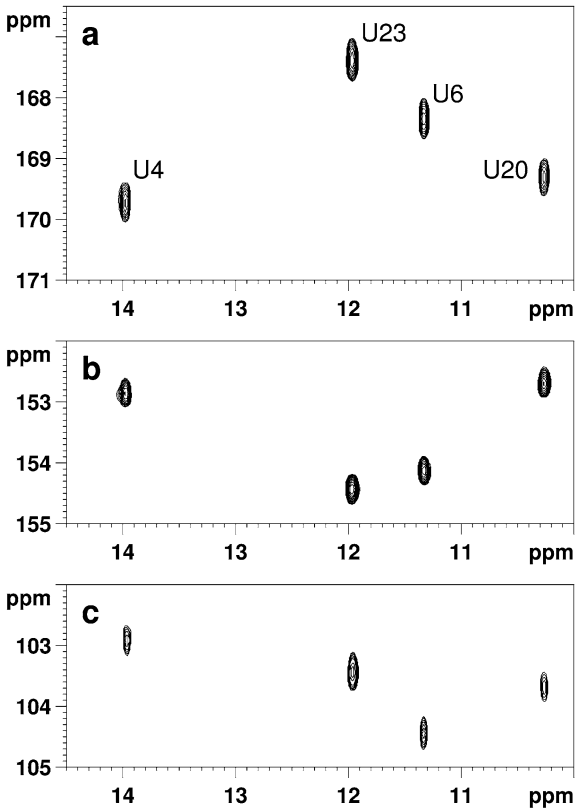

Figure 7. Uracil H3-C2 (a), H3-C4 (b) and H3-C5 (c) correlations using the HNC experiment. The selectivity of the nitrogen-carbon polarization transfer was achieved by 2.245 ms and 2.0 ms Q3 pulses applied to nitrogen and carbon, respectively, in the middle of the evolution periods. For the H3-C4 and H3-C5 correlations, the effect of the carbon-carbon couplings was removed by the constant-time evolution in t_1. For other experimental parameters, see Table 1.

lations show a rather large J_{N1C5} coupling of 8.4 Hz, which indicates that the polarization transfer between N1 and C5 should be possible. While the C2 carbon does not have a large one bond coupling to another carbon, the C6 is coupled to the C5 and the C5 is coupled to both the C4 and the C6. Therefore, different strategies were employed for the t_1 evolution period. For the H1-C2 correlation, a simple t_1 evolution as shown in Figure 2b is adequate. In the H1-C6 experiment, the constant time evolution was used, and for the H1-C5 correlation, the carbon-carbon coupling was eliminated by a selective inversion of the C4 and C6 magnetization (Figure 2d). The guanine H1-C2 and H1-C6 correlations (Figures 5a, b) provide spectra of an excellent quality with a high signal-to-noise ratio. The imino protons exhibit typically a very good dispersion of the chemical shifts and the peaks overlap is not a problem. On the other hand, some of the imino protons are usually not detectable due to the exchange broadening. We have obtained signals from five out of eight guanine residues in the molecule, missing the peaks from the terminal residues (G1, G2) and from the non-paired G13 in the loop. The experiment has confirmed that indeed the J_{N1C5} coupling can be used to obtain the H1-C5 correlation peaks (Figure 5c). The peaks are of a noticeably lower intensity than those in the H1-C6 spectrum, though, indicating that the calculated value of the J_{N1C5} coupling is probably somewhat overestimated.

The pyrimidine bases have two quaternary carbons, namely C4 and C2. The three bond couplings of these carbons to H6 ($\sim$8 Hz in uracil, $\sim$6 Hz in cytosine) enable a direct correlation using a selective long-range HSQC experiment (Figures 6a, c) similar to the purine H8-C4 and the H8-C5 correlation. In the case of C4, the large one-bond coupling to the C5 was eliminated by a selective refocusing (Figure 2d). Since there are no significant long-range carbon-carbon couplings in the pyrimidine nucleotides, the constant time evolution would be equally effective in this case. The sensitivity of the H6-C4 and H6-C2 experiments is good. However, a limited dispersion of chemical shifts in both dimensions leads to frequent peak overlaps.

Alternatively, the H6-C2 correlation can be obtained using the H(CN)C experiment based on the consecutive H8-C6, C6-N1 and N1-C2 steps (Figure 2c). The experiment is virtually identical to the one described for the H8-C4 correlation in purines, except that it does not require a provision for eliminating the carbon-carbon couplings in the t_1 period. In cytosine, both C6-N1 and N1-C2 couplings are around 12 Hz. In uracil, the N1-C2 coupling is close to 20 Hz, which leads to some loss of signal when $2N1_xC2_z$ magnetization is evolving and $2N1_xC6_z$ is being refocused at the same time. The resulting spectrum (Figure 6d) exhibits a lower sensitivity compared to the LR-HSQC spectra based on the H6-C2 coupling. An advantage of the H(CN)C approach is that the peaks from pyrimidine and purine residues can be easily separated based on different N1/9 resonance frequencies.

Instead of the H6, pyrimidine C4 carbon can be correlated to the H5 proton using the H(C)C experiment (Figure 6b). In this case, the experiment is significantly more sensitive than when used for the purine H8-C4 correlation since it relies here on a large one-bond J_{C5C4} coupling (55 Hz for cytosine, 65 Hz for uracil). The polarization transfer from C5 to C4 was achieved by a nonselective 180° pulse while

the selective inversion pulses applied at the C6 carbon resonance blocked the unwanted C5 to C6 path (Figure 2a, inset).

In uracil, the quaternary carbons can also be correlated to the imino proton using the H(N)C experiment (Figure 2b) in a way similar to guanine H1-C2 and H1-C6 experiments. Thanks to the large $^1J_{N3C2}$ (19.2 Hz) and $^1J_{N3C4}$ (10.7 Hz) couplings, the experiments provide excellent sensitivity (Figure 7a, b). For the $^2J_{N3C5}$ coupling, the *ab initio* calculations predict the values of −10.3 Hz and −7.2 Hz for a free and a base-paired 1-methyluracil, respectively. These are noticeably larger values than 5.7 Hz measured on 5′-UMP (Wijmenga and van Buuren, 1998). A simple fitting of the peak intensities in H3-C5 correlation spectra measured with four different evolution intervals Δ (Figure 2b) provided $^2J_{N3C5}$ for individual signals in the range 5.8 Hz to 8.4 Hz with an average value of 7.3 Hz. A simulated relaxation rate of 8.3 s^{-1} for the magnetization effective during the evolution was used for the fitting. Because of a much smaller coupling and a faster relaxation during the t_1 period, the H3-C5 correlation spectra (Figure 7c) exhibit a considerably lower sensitivity than the H3-C2 and H4-C4 correlations. Because of a better dispersion of the imino proton chemical shifts compared to H6, the H(N)C experiments are preferable for the uracil residues whose imino proton resonances are not broadened by an exchange.

We have performed an analysis of the sensitivity of the experiments by comparing the experimental performance to the relative sensitivity simulated based on the lengths of the evolution intervals, the couplings involved and the relaxation rates of the active magnetizations. The relative simulated and experimental sensitivities, normalized to the intensity of the most sensitive H3-C2 HNC correlation experiment in uracil, are summarized in Table 2. The simulated intensities were calculated from the efficiencies of each individual polarization transfer step in the pulse sequence expressed as

$$I = I_0 \prod_i p \sin(\pi J_i t_i) \exp(-R_{2,i} t_i), \qquad (1)$$

where J_i, t_i and $R_{2,i}$ are the coupling constants, durations and the relaxation rates effective in the consecutive evolution periods, respectively. The parameter p characterizes instrumental imperfections affecting the efficiency of the polarization transfer and its value was set to 0.9. The lengths of the constant time interval were taken into account as well. The relaxation rates were calculated as described in Supplementary material. The experimental sensitivities were measured as signal-to-noise ratios averaged over all the peaks in the spectrum.

Table 2. Calculated and experimental relative sensitivities of the long-range HSQC, HCC, HNC and HCNC experiments applied to correlations of quaternary carbons in RNA bases

Correlation experiment	RS^{sim}	RS^{exp},iso	S_{peg}/S_{iso}
Adenine H2-C4 HSQC	0.38	0.83	0.23
Adenine H8-C4 HSQC	0.07	0.15	0.24
Adenine H2-C6 HSQC	0.36	0.35	
Purine H8-C5 HSQC	0.26	0.63	0.23
Purine H8-C4 HCC	0.11	0.20	0.77
Purine H8-C4 HCNC	0.11	0.11	0.36
Pyrimidine H6-C2 HSQC	0.10	0.53	0.46
Pyrimidine H6-C2 HCNC	0.07	0.15	0.55
Pyrimidine H6-C4 HSQC	0.10	0.42	0.66
Pyrimidine H5-C4 HCC	0.84	0.41	0.66
Guanine H1-C2 HNC	0.77	0.49	
Guanine H1-C6 HNC	0.32	0.33	
Guanine H1-C5 HNC	0.38	0.12	
Uracil H3-C2 HNC	1.00	1.00	0.40
Uracil H3-C4 HNC	0.59	0.52	0.42
Uracil H3-C5 HNC	0.34	0.16	

RS^{sim} – simulated relative sensitivity of the correlation experiments calculated using Equation 1. Details of the simulations are available as Supplementary material.
RS^{exp},iso – experimental relative sensitivity in the isotropic phase.
S_{peg}/S_{iso} – experimental sensitivity in the oriented phase relative to the sensitivity of the same experiment in the isotropic phase

The simulation correctly predicts the uracil H3-C2 HNC correlation as the most sensitive experiment. Some other experiments, however, exhibit sensitivities significantly different from those predicted theoretically. Most notably, the long-range HSQC experiments perform much better than theoretically predicted. This result indicates that the efficiency of the experiments based on complicated polarization transfer pathways, including the H(N)C H3-C2 correlation used as a standard, suffers. The HSQC experiments consist of only 11 pulses. In contrast, the H(C)C comprises 15 or 17 pulses, the H(N)C 19 pulses, and the H(CN)C experiment as many as 29 pulses. This is a significant difference even if the imperfections of the individual pulses are small. The results highlight the importance of a well known, but sometimes overlooked, principle that experiments with fewer pulses perform in general better than their more complicated counterparts.

To verify the applicability of the experiments described above to the measurements of the chemical

shift changes induced by the orientation of the molecules in the magnetic field we have also tested the performance on a sample containing an oriented phase (polyethylene glycol). In practice, the sensitivity of experiments performed on such samples is limited largely by the broadening of the proton resonances due to the ^{1}H-^{1}H dipolar interactions. The experiments relying on long evolution periods involving the proton transverse magnetization are particularly sensitive to such interference. As a result, the sensitivity considerations mentioned above change somewhat in the oriented media. As summarized in Table 2, the HSQC experiments exhibit a notable loss in sensitivity. On the other hand, the experiments where the longest magnetization-transfer steps involve carbon and/or nitrogen nuclei are affected to a lesser extent. Therefore the availability of several approaches for achieving a particular type of correlation represents a considerable advantage. The best option can be chosen based on the specific experimental conditions.

Conclusions

We have presented a set of two-dimensional correlation experiments that make possible to assign and measure chemical shifts of all quaternary carbon atoms in RNA bases. The only remaining issue is the C2 carbons of the guanine residues whose imino protons are broadened beyond detection. The sensitivity of all the experiments described was high enough to obtain a spectrum of 0.5 mM 25-mer RNA stem-loop in four hours or less on a 600 MHz (^{1}H) spectrometer. For molecules significantly larger than used here and at very high magnetic fields, the pulse sequences involving extensive evolution periods of ^{13}C or ^{15}N magnetization could employ the multiple-quantum narrowing (Griffey and Redfield, 1987) or TROSY (Pervushin et al., 1997) which would likely provide superior sensitivity at these conditions. The experiments are applicable to samples containing agents for a weak molecular alignment as well.

The *ab initio* calculations of the coupling constants in the free bases and the AU and GC base pairs complement the experimental values, resolve the ambiguities in the assignment of some CN couplings in guanine and reveal surprisingly high values of guanine $^{2}J_{N1C5}$ and uracil $^{2}J_{N3C5}$ couplings. Significant values of the couplings have been confirmed experimentally. The theoretical results demonstrate that there is a significant influence of base pairing on the spin-spin couplings. The sensitivity to base pairing and the agreement with experiment obtained depend strongly on the type of nuclei involved and the number of bonds separating them. Particular types of coupling reveal similar performance for all bases in question. In many cases, the experimental data obtained for mononucleosides compare better to the theoretical data for the base pairs than to those for isolated bases.

In the final stages of the manuscript preparation, we learnt about a paper in press that deals in part with the same topic (Fürtig et al., 2004). The authors suggest an HNC6C5 experiment for correlating purine C5 to the imino proton. We have found that the assignment of C5 in purines by correlating it to H8 is so straightforward thanks to a rather large $^{3}J_{H8C5}$ coupling ($\sim$11 Hz) that we felt no need for additional experiments. In guanine, there is also an option to make a direct N1-C5 transfer using the H(N)C experiment. However, this is a less sensitive alternative and the main reason we performed the experiment was to verify the existence of the calculated J_{N1C5} coupling. Both Schwalbe's and our groups propose the H(CN)C experiment for correlating H8 to C4 in purines and H6 to C2 in pyrimidines. The pulse sequences designed follow essentially the same philosophy and differ only in technical details. In our experience, though, the H(C)C experiment for the H8-C4 correlation in purines, the LR-HSQC for the H2-C4 correlation in adenine and the H6-C2 correlation in pyrimidines, as well as the H3-C2 correlation in uracil, all provide sensitivity superior to the H(CN)C experiment and should be preferred in most circumstances.

Supplementary material available: Equations used for calculating the relaxation rates and tables of *ab initio* calculated chemical shift anisotropies and coupling constants; http://kluweronline.com/issn/0925-2738

Acknowledgements

The work was supported by the grant LN00A016 provided by the Ministry of Education of the Czech Republic. We are indebted to Sam Butcher for providing the samples and for the spectra assignments, and to Harald Schwalbe for making available a preprint of his paper.

References

Altona C., Faber D.H., and Hoekzema A.J.A.W. (2000) *Magn. Reson. Chem.*, **38**, 95–107.
Becke, A.D. (1988) *Phys. Rev. A*, **38**, 3098–3100.
Becke, A.D. (1993) *J. Chem. Phys.*, **98**, 5648–5652.

Boisbouvier, J., Delaglio, F. and Bax, A. (2003) *Proc. Natl. Acad. Sci. USA*, **100**, 11333–11338.

Brutscher, B., Boisbouvier, J., Kupče, E., Tisné, C., Dardel, F., Marion, D. and Simorre, J.P. (2001) *J. Biomol. NMR*, **19**, 141–151.

Cavanagh, J., Fairbrother, W.J., Palmer, A.G. and Skelton, N.J. (1996) *Protein NMR Spectroscopy: Principles and Practice*, Academic Press, San Diego, p. 269.

Cromsigt, J., Hilbers, C.W. and Wijmenga, S.S. (2001) *J. Biomol. NMR*, **21**, 11–29.

Dingley, A.J. and Grzesiek, S. (1998) *J. Am. Chem. Soc.*, **120**, 8293–8297.

Emsley, L. and Bodenhausen, G. (1992) *J. Magn. Reson.*, **97**, 135–148.

Farmer, B.T., Muller, L., Nikonowicz, E.P. and Pardi, A. (1994) *J. Biomol. NMR*, **4**, 129–133.

Fiala, R., Czernek, J. and Sklenář, V. (2000) *J. Biomol. NMR*, **16**, 291–302.

Fiala, R., Jiang, F. and Patel, D.J. (1996) *J. Am. Chem. Soc.*, **118**, 689–690.

Frisch, M.J., Pople, J.A. and Binkley, J.S. (1984) *J. Chem. Phys.*, **80**, 3265–3269.

Frisch, M.J., Trucks, G.W., Schlegel, H.B., Scuseria, G.E., Robb, M.A., Cheeseman, J.R., Zakrzewski, V.G., Montgomery, J., J.A., Stratmann, R.E., Burant, J.C., Dapprich, S., Millam, J.M., Daniels, A.D., Kudin, K.N., Strain, M.C., Farkas, O., Tomasi, J., Barone, V., Cossi, M., Cammi, R., Mennucci, B., Pomelli, C., Adamo, C., Clifford, S., Ochterski, J., Petersson, G.A., Ayala, P.Y., Cui, Q., Morokuma, K., Malick, D.K., Rabuck, A.D., Raghavachari, K., Foresman, J.B., Cioslowski, J., Ortiz, J.V., Baboul, A.G., Stefanov, B.B., Liu, G., Liashenko, A., Piskorz, P., Komaromi, I., Gomperts, R., Martin, R.L., Fox, D.J., Keith, T., Al-Laham, M.A., Peng, C.Y., Nanayakkara, A., Gonzalez, C., Challacombe, M., Gill, P.M.W., Johnson, B., Chen, W., Wong, M.W., Andres, J.L., Gonzalez, C., Head-Gordon, M., Replogle, E.S. and Pople, J.A. (1998) Gaussian 98 (Revision A.9), Gaussian, Inc., Pittsburgh, PA.

Fürtig, B., Richter, C., Bermel, W. and Schwalbe, H. (2004) *J. Biomol. NMR*, **28**, 69–79.

Geen, H. and Freeman, R. (1991) *J. Magn. Reson.*, **93**, 93–141.

Griffey, R.H. and Redfield, A.G. (1987) *Q. Rev. Biophys.*, **19**, 51–82.

Grzesiek, S. and Bax, A. (1993) *J. Am. Chem. Soc.*, **115**, 12593–12594.

Hehre, W.J., Ditchfield, R. and Pople, J.A. (1972) *J. Chem. Phys.*, **56**, 2257–2261.

Hennig, M., Carlomagno, T. and Williamson, J. R. (2001) *J. Am. Chem. Soc.*, **123**, 3395–3396.

Hu, W.D., Gosser, Y.Q., Xu, W.J. and Patel, D.J. (2001) *J. Biomol. NMR*, **20**, 167–172.

Kay, L.E., Ikura, M. and Bax, A. (1990) *J. Am. Chem. Soc.*, **112**, 888–889.

Krishnamurthy, V.V. (1996) *J. Magn. Reson. B*, **112**, 75–78.

Kutzelnigg, W., Fleischer, U. and Schindler, M. (1990) *NMR – Basic Principles and Progress*, **23**, 167–262.

Majumdar, A. and Patel, D.J. (2002) *Accounts Chem. Res.*, **35**, 1–11.

Majumdar, A., Gosser, Y. and Patel, D.J. (2001) *J. Biomol. NMR*, **21**, 289–306.

Malkin, V.G., Malkina, O.L., Casida, M.E. and Salahub, D.R. (1994a) *J. Am. Chem. Soc.*, **116**, 5898–5908.

Malkin, V.G., Malkina, O.L., Eriksson, L.A. and Salahub, D.R. (1994b) In *Theoretical and Computational Chemistry*, Vol. 2, Seminario, J. M. and Politzer, P. (Eds.), Elsevier, Amsterdam, pp. 273–401.

Marion, D., Ikura, M. and Bax, A. (1989) *J. Magn. Reson.*, **84**, 425–430.

Muhandiram, D.R. and Kay, L.E. (1994) *J. Magn. Reson. B*, **103**, 203–216.

Munzarová, M.L., Sklenář, V. (2002) *J. Am. Chem. Soc.*, **124**, 10666–10667.

Padrta, P., Štefl, R., Králík, L., Žídek, L. and Sklenář, V. (2002) *J. Biomol. NMR*, **24**, 1–14.

Peng, J.W. and Wagner, G. (1994) In *Methods in Enzymology*, Vol. 239: *Nuclear Magnetic Resonance*, Part C, James, T.L. and Oppenheimer, N.J. (Eds.), Academic Press, San Diego, pp. 563–596.

Perdew, J.P. (1986a) *Phys. Rev. B*, **34**, 7406–7406.

Perdew, J.P. (1986b) *Phys. Rev. B*, **33**, 8822–8824.

Perdew, J.P. and Wang, Y. (1986) *Phys. Rev. B*, **33**, 8800–8802.

Pervushin, K. (2001) *J. Biomol. NMR*, **20**, 275–285.

Pervushin, K., Ono, A., Fernandez, C., Szyperski, T., Kainosho, M. and Wüthrich, K. (1998) *Proc. Natl. Acad. Sci. USA*, **95**, 14147–14151.

Pervushin, K., Riek, R., Wider, G. and Wüthrich, K. (1997) *Proc. Natl. Acad. Sci. USA*, **94**, 12366–12371.

Phan, A.T. (2000) *J. Biomol. NMR*, **16**, 175–178.

Phan, A.T. (2001) *J. Magn. Reson.*, **153**, 223–226.

Piotto, M., Saudek, V. and Sklenář, V. (1992) *J. Biomol. NMR*, **2**, 661–665.

Richter, C., Reif, B., Griesinger, C. and Schwalbe, H. (2000) *J. Am. Chem. Soc.*, **122**, 12728–12731.

Salahub, D.R., Fournier, R., Mlynarski, P., Papai, I., St-Amant, A. and Ushio, J. (1991) In *Density Functional Methods in Chemistry*, Labanowski, J. and Andzelm, J. (Eds.), Springer, New York.

Shaka, A.J., Barker, P.B. and Freeman, R. (1985) *J. Magn. Reson.*, **64**, 547–552.

Simon, B., Zanier, K. and Sattler, M. (2001) *J. Biomol. NMR*, **20**, 173–176.

Simorre, J.P., Zimmermann, G.R., Mueller, L. and Pardi, A. (1996) *J. Biomol. NMR*, **7**, 153–156.

Sklenář, V., Dieckmann, T., Butcher, S.E. and Feigon, J. (1996) *J. Biomol. NMR*, **7**, 83–87.

Sklenář, V., Peterson, R.D., Rejante, M.R. and Feigon, J. (1993) *J. Biomol. NMR*, **3**, 721–727.

Sklenář, V., Peterson, R.D., Rejante, M.R. and Feigon, J. (1994) *J. Biomol. NMR*, **4**, 117–122.

Wijmenga, S.S. and van Buuren, B.N.M. (1998) *Prog. Nucl. Magn. Reson. Spectrosc.*, **32**, 287–387.

Wijmenga S.S, Kruithof M., and Hilbers C.W. (1997) *J. Biomol. NMR*, **10**, 337–350.

Wishart, D.S., Bigam, C.G., Yao, J., Abildgaard, F., Dyson, H.J., Oldfield, E., Markley, J.L. and Sykes, B.D. (1995) *J. Biomol. NMR*, **6**, 135–140.

Wohnert, J., Gorlach, M. and Schwalbe, H. (2003) *J. Biomol. NMR*, **26**, 79–83.

Wohnert, J., Ramachandran, R., Gorlach, M. and Brown, L.R. (1999) *J. Magn. Reson.*, **139**, 430–433.

Wu, Z.G., Delaglio, F., Tjandra, N., Zhurkin, V.B. and Bax, A. (2003) *J. Biomol. NMR*, **26**, 297–315.

Wu, Z.R., Tjandra, N. and Bax, A. (2001a) *J. Biomol. NMR*, **19**, 367–370.

Wu, Z.R., Tjandra, N. and Bax, A. (2001b) *J. Am. Chem. Soc.*, **123**, 3617–3618.

Yan, J.L., Corpora, T., Pradhan, P. and Bushweller, J.H. (2002) *J. Biomol. NMR*, **22**, 9–20.

Žídek, L., Wu, H.H., Feigon, J. and Sklenář, V. (2001) *J. Biomol. NMR*, **21**, 153–160.